System Reliability Analysis Of A Tension Leg Platform

Qian Ye[1*], Wei-liang Jin[2], and Yong Bai[2]

[1] School of Civil Engineering and Architecture, Taizhou University, Jiaojiang 318000, Zhejiang Province, China;
[2] Department of Civil Engineering, Zhejiang University, Hangzhou 310000, Zhejiang Province, China
[*] Corresponding author. E-mail: geneye@tzc.edu.cn

Received: Mar. 21, 2022; Accepted: Nov. 29, 2022

For the overall safety evaluation of the tension leg platform (TLP) system, the structural strength reliability analysis is essential. The strength reliability of a typical TLP exposed to combined static and extreme wave loads is the subject of this study. A three-dimensional finite element shell model made up of a pontoon, column, and deck that is assumed to be accurate and efficient with tendon system as the boundary conditions was built using a concrete TLP. By employing the proportional loading method based on the design wave method, failure mechanisms for the platform and were determined. The failure mechanisms were then used to derive limit state expressions. The system reliability indexes of the object platform were calculated using the system reliability assessment framework created by the system reliability model suggested in this paper. This work seeks to advance the application of reliability theory in offshore engineering.

Keywords: Tension leg platform; System reliability; Finite element method; Numerical simulation; Failure probability
© The Author('s). This is an open-access article distributed under the terms of the Creative Commons Attribution License (CC BY 4.0), which permits unrestricted use, distribution, and reproduction in any medium, provided the original author and source are cited.
http://dx.doi.org/10.6180/jase.202401_27(1).0013

1. Introduction

The consumption of oil and natural gas has increased as a result of the rise in global demand. The world is paying more attention to marine oil resources as a result of the depletion of continental oil resources. As a result, a number of innovative marine structures are emerging. The marine environment is very unforgiving and unpredictable. Therefore, the conventional techniques for designing and analyzing structures constructed in the marine environment occasionally produce unreliable results. By taking into account the impact of uncertainties in material and load parameters, the reliability design method, in contrast to conventional design methods, can improve the safety and economy of marine structures. One of the most important issues in the field of offshore engineering is always the system reliability. Nearly forty years ago, the offshore engineering community started to pay attention to this problem. The literature on this topic at the time was reviewed and compiled in 1983 by the structural reliability committee of the American Society of Civil Engineers (ASCE) [1]. In the reliability analysis of nonlinear systems that followed, Wu and Moan [2] presented an incremental load formulation for limit states. Utilizing a differential incremental load formulation that took into account random stiffness and strength, limit states were created.

A methodology for the time-variant reliability assessment of floating production storage and offloading (FPSO) hull girders subject to degradations due to corrosion and fatigue was presented by Sun and Bai [3]. A technique for the reliability-based design of ship structures was created by Soares et al. [4]. Purnenduetc and Das [5] also concentrated on the evaluation of FPSO reliability. In addition, the ultimate strength of stiffened panels corresponding to various failure modes was examined by He and Xu [6]. The reliability method was used to conduct the safety assessments of the stiffened panel and the ultimate limit state (ULS) equations. Low [7] used the frequency domain analysis technique to ascertain the tendon restoring forces of a TLP. Moreover, the proposed method of identifying dominant failure modes is decoupled from system-level reliability analyses was used by Lee and Song [8]. This method avoids performing reliability analyses repeatedly throughout the identification process, but it may result in significant computational costs, particularly for large and highly redundant structures. Ye et al. [9] discussed system reliability analysis techniques for a semi-submersible drilling rig and used a series calculation model to find a solution,[10, 11] conducted researches on TLP's hydrodynamic response and global strength. Furthermore, a TLP was experimentally studied by Jin et al. [12] under wave and flow conditions at various heading angles, and the most unfavorable heading angle was suggested. Their research laid a solid foundation for future research on the structural behavior of Coccon et al. [13] proposed an effective and precise method for risk assessment of offshore structures, estimated with respect to the system-level failure caused by possible failure modes consisting of component failures with their statistical dependence taken into consideration, and presented the method using a Jacket platform.

Wave loads dominate the behavior of structures,[14–16] conducted some experiments. The test data were compared with the results of the numerical simulations, and good agreements were found. The main goal of this paper is to address the system reliability of a tension leg platform under extreme sea states, in which uncertainties are assumed with regard to the wave and hydrodynamic model as well as the material properties of the structural members. This work also proposes system reliability methods and discusses their applicability and merits. Consideration is given to the example of a TLP under heavy sea loading. The probabilistic model of the extreme sea loading is derived from a short-term design storm using Thoft-Christensen and Murotsu's method [17], in which uncertainties are assumed for both the wave model and the hydrodynamic model. Through a case study of a specific TLP, the computational effectiveness and accuracy of the suggested approach are successfully illustrated.

2. Finite element model of tlp

A typical TLP serves as the object platform for this study. It has columns separating the four parallel pontoons. The finite element software ANSYS was used to create a finite element model that accurately represented the structure behavior.

2.1. Geometric of the object platform

The main dimensions of a typical TLP are listed in Table 1, and Fig. 1 displays the main structure's dimensions, including the pontoons, columns, and deck as well as how they relate to one another.

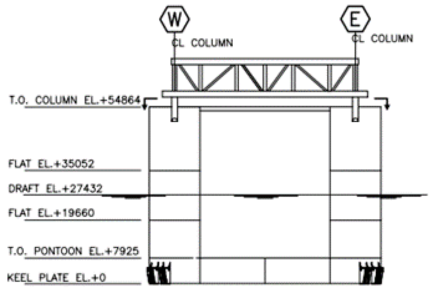

Fig. 1. Concept map of TLP

2.2. Material properties

The structure and behavior of TLP are dominated by the stress versus strain relationship. The elastic-perfectly plastic material model is used in this study without taking into account the impact of strain hardening. EQ36 is chosen for the entire structure with a yield stress of 355 MPa, a Young's modulus E of 206 GPa, and a Poisson's ratio of 0.3, because the majority of the platform structure is made of EQ36 and only a small portion of the structure, is made of EQ56 for transition.

2.3. Loading condition

After the generation of the wave load, the load condition will be determined. Using the wave analysis program WAMIT, a linear 3D frequency-domain method was used to determine the hydrodynamic load. The focuses are subjected to the typical hydrodynamic wave load as the center hold gradually collapses.

2.4. Nonlinear finite element mesh modeling

The finite element software ANSYS is used to construct the nonlinear finite element model for the object platform. Fig. 2 depicts the model that was used in the present study. The platform's main framework is made up of a pontoon, a column, and a deck. Each of their components can be broken down into smaller structural components like a bulkhead, girder, stiffener, etc. A large volume, thin-walled, three-dimensional shell model (represented by area) in conjunction with a beam model should be used to represent the global FE-model, which shall represent the global stiffness of the structure (represented by line). Connections, such as those between a pontoon and a column or between a column and a deck, are crucial components of the TLP. These connections are adequately depicted in detail.

Studies on mesh convergence have been done for the entire model, with a focus on the crucial (connection) region. Mesh sizes around 0.5 m are used for connections,

Table 1. Configurations of the object platform

Properties	Parameters m	Properties	Parameters(m)
Column height	54.864	Adjacent column distance	56.388
Column radius	8.914	Inner shell radius of column	3.658
Upper partition height	15.392	Lower partition height	27.925
Middle partition height	11.735	Depth of draught	
Pontoon Height	7.925	Tension leg length	1272.846
Float box width	8.622	Deck height	

Table 2. Design wave parameters of 100 return periods

Load case	Wave load type	Wave periodic	Incident direction	Wave amplitude	Phase angle
1	Longitudinal extrusion	6 s	0°	5.4 m	160.2°
2	Oblique compression	8*s*	45°	4.4 m	33.8°
3	Maximum acceleration	18 s	0°	6.35 m	−128°
4	Topside shearing	6 s	180°	4.7 m	130°

and other areas of the platform have mesh that is roughly 1 to 1.5 m in size. There are five different types of element types (e.g., shell 181, beam 188, mass 21, combine 14, pipe 289). The DNV rules' recommendations served as the basis for the mesh size, elements, and element type used in this paper. The mesh strategy is thought to be capable of capturing realistic structure behavior of the platform with appropriate computational time and requirements on the computer's capacity based on trial and error test analyses. About 240 000 elements make up the entire model.

Tendon is used as the boundary conditions for the finite element model in accordance with the DNV rules. The object platform's finite element model is depicted in Fig. 2.

3. Structural responses of tlp

3.1. Structural analysis method of TLP

For the complex dynamic problem such as structural responses of TLP in harsh marine environment, it is important to consider ambient loads, such as external pressure loads, mass-acceleration terms, and additional loads. The exterior loading factors result in external pressure loads, and the motion of the vessel results in mass-acceleration terms. Hydrodynamic analysis is typically used to determine these two types of loads. Live loads and other additional loads are typically regarded as insignificant for global stress and are not included in the motion analysis. These loads might be crucial for the local structure. The floating structure is significantly affected by mass effects. Structural mass equipment loads, personnel, stores, fuel, and other terms should be mentioned. Unrealistic point reactions are the result of an unequal distribution of masses or large lumped masses. Structure and other masses should therefore be dispersed over appropriate areas. Typically, artificially increasing the structural steel density by region is used to address this issue. Additionally, hydrodynamic and structural analysis both require identical masses to be represented. The centroid and second moment of mass about each axis should also be as accurate as possible due to assumptions used in the hydrodynamic analysis.

3.2. Ultimate limit state analysis of TLP

Cases analysis exposed to typical hydrodynamic circumstances were carried out without taking geometric nonlinearity and imperfection into account. The method for assessing the ultimate limit state, shown in Fig. 3, was used to calculate the progressive collapse of the object platform. Fig. 4 illustrates the various collapse modes that were seen. The platform structure's deformed shapes and von-Mises stress distributions at the ultimate limit state under typical wave load conditions reveal how the TLP structure gradually failed.

3.3. Ultimate limit state expression of TLP

The main section load of the corresponding load case was closely related to the ultimate limit state of TLP. The proposed ultimate limit state expression for the ultimate limit state design, which was based on the main section load, is as follows:

$$Z = \gamma_u R_u - \gamma_w \gamma_m S_w \tag{1}$$

where γ_u denotes uncertainties related to the wave model, R_u denotes the platform's ultimate strength, S_w denotes the load effect on the platform's random variable denoting the wave-induced tension (or compression) force, and γ_m denotes model uncertainties for deducing the strength of TLP.

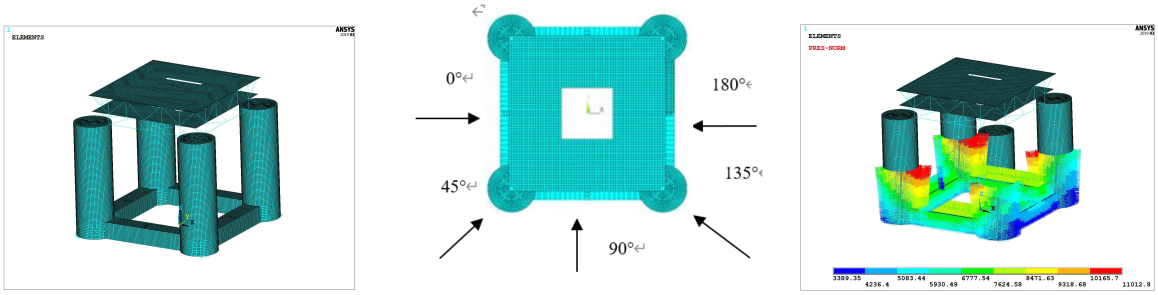

Finite element model
a

Different heading angles
b

Characteristic wave loads
c

Fig. 2. A nonlinear FEM and wave conditions for the object platform

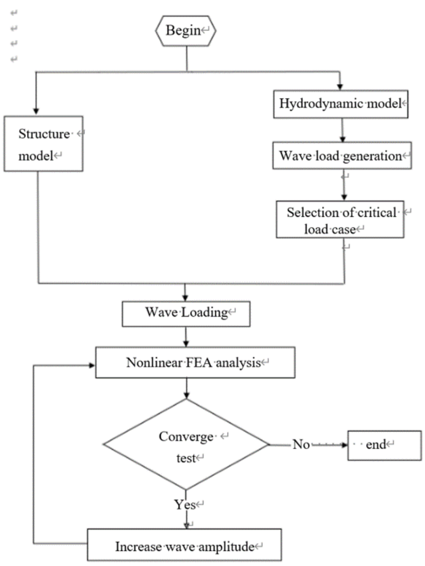

Fig. 3. Flow chart of numerical solution procedure for global ultimate strength assessment

4. System reliability method of tension leg platform

4.1. Methods for system reliability analysis

The challenge of dealing with uncertainty is at the heart of the structural reliability issue. The likelihood of performing a specific preset function within the allotted time under the allotted conditions is known as structural reliability. In contrast, the corresponding probability is known as structural failure probability if the structure fails to perform a specific predetermined function. Failure and structural reliability are two occurrences that cannot coexist. As a result, failure probability and structural reliability probability work together.

When conducting a structural reliability analysis, structural failure probability is frequently used as a proxy for structural reliability to facilitate calculation and expression. Calculating structural failure probability in accordance with the statistical properties of random variables and the limit state equation of the structure forms the basis of structural reliability analysis.

In structural reliability analysis, a function typically describes the structure's operational state. When random factors have an impact on structural reliability, Eq. (1) describes the structure's operational state.

$$Z = g\left(x_1, x_2 \ldots x_n\right) \begin{cases} < 0 \text{ failure state} \\ = 0 \text{ limit state} \\ > 0 \text{ reliable state} \end{cases} \tag{2}$$

If the structure succeeds in performing its current function under the given conditions, the corresponding probability is known as the structural failure probability, and is represented by P_s. If the structure fails to perform its current function, the corresponding probability is known as the structural failure probability, and is represented by P_f. Failure and structural reliability are two events that are mutually exclusive and have a complementary relationship, i.e. $P_s + P_f = 1$

Because structural failure has a low probability of occurring (P_f is typically less than 0.001), it is frequently measured in terms of structural reliability for ease of calculation and expression.

Let $f\left(x_1, x_2 \ldots x_n\right)$ be the joint probability density function for the structure's fundamental random variable $X = \left(x_1, x_2 \ldots x_n\right)^T$. Eq. (2) is used to represent the structural function. Structural failure probability can be expressed as Eq. (3) in accordance with the definition of structural reliability and the fundamental idea of probability theory.

$$P_f = P(Z < 0) = \iint_{Z<0} \int f\left(x_1, x_2 \ldots x_n\right) dx_1 dx_2 \ldots dx_n \tag{3}$$

However, in actual calculations, when there are numerous basic random variables present in the function, the

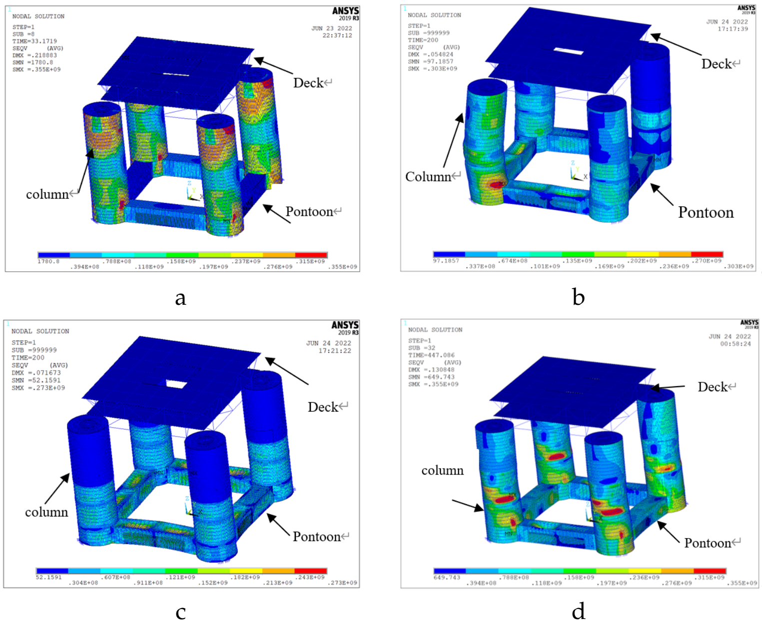

Fig. 4. Ultimate limit states of TLP

limit state function is nonlinear and the variables are not independent of one another, making it challenging to directly solve the equation above. As a result, this direct integration approach is rarely used. Instead, a straightforward approximation method is used, and for all random variables, only their digital eigenvalues are taken into account. Mean and variance are used to describe the statistical properties of these variables. The corresponding failure probability is therefore computed by introducing and using the reliability index.

Let's first assume that the function variable has a mean of and a mean-square error of under a normal distribution. The following is its probability density function:

$$f(z) = \frac{1}{\sigma_z\sqrt{2\pi}} \exp\left[-\frac{1}{2}\left(\frac{z-\mu_z}{\sigma_z}\right)^2\right] \quad (4)$$
$$-\infty < z < +\infty$$

In Fig. 5, the dashed area represents the likelihood of structural failure. The failure probability is expressed as follows

$$P_f = \int_{-\infty}^{0} f(z)dz = f(z) = \frac{1}{\sigma_z\sqrt{2\pi}} \exp\left[-\frac{1}{2}\left(\frac{z-\mu_z}{\sigma_z}\right)^2\right] dz = \frac{1}{\sqrt{2\pi}} \exp\left[\left(-\frac{t^2}{2}\right)\right] dt = \Phi\left(\frac{\mu_z}{\sigma_z}\right) \quad (5)$$

Notation β is introduced. Let

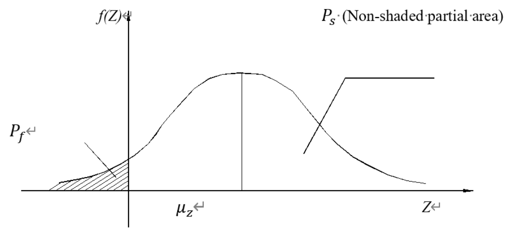

Fig. 5. Diagram of structural failure probability

$$\beta = \frac{\mu_z}{\sigma_z} \quad (6)$$

Eq. (6) can be converted into

$$P_f = \Phi(-\beta) \quad (7)$$

The relationship between β and reliability can be expressed by the following equation:

$$P_s = 1 - P_f = 1 - \Phi(-\beta) = \Phi(\beta) \quad (8)$$

where, the reliability index mentioned above is the equation's dimensionless coefficient β. In terms of structural reliability, it can be written as

$$P = P(Z < 0) = \int_{D_f} f(X)dX \quad (9)$$

$$\beta = -\Phi^{-1}\left(P_f\right) \quad (10)$$

where, $Z = G(X)$ is the critical state, $Z < 0$ (failure), while $Z > 0$ (safety), and $Z = 0$ is the critical state. D_f

represents the failure zone corresponding to $Z < 0$, and $f(X)$ represents the joint probability density function of random variables.

Therefore, the following four issues should be addressed using the structural reliability theory:

1. In accordance with the random theory, various design parameters are converted into random variables. Additionally, the relevant probability distribution (including the type of distribution and statistical parameters) is established. These are issues with statistical analysis because the random variables are not statistically independent, so it is necessary to ascertain their joint distribution.

2. In order to create a useful limit state equation functions made up of fundamental variables and definite quantities are chosen in accordance with the design specifications. The issue with setting up a structural failure model is $Z = G(X)$, where $Z < 0$ represents failure while $Z \geq 0$ represents safety; where $g(x)$ represents a function space composed of a single limit state function, and $G(X)$ means that it is composed of multiple limit state functions.

3. When a multi-dimensional integral problem is solved within D_f, it is possible to obtain the corresponding failure probability; this is a numerical analysis issue.

4. Structure reliability is divided into the reliability of the component and system levels, and an allowable failure probability value will be set for various structures and their corresponding limit states, which may involve economic and social benefits.

Because a structure's system frequently consists of multiple components, system reliability is much more complicated than component level reliability [18]. A general failure model of the structural system is shown in Fig. 5 with various failure paths, including 1, 2, and K. Each failure path is assumed to be made up of a number of parallel failure elements. A structure's failure path, failure element, and relationships between each component and system reliability can all be clearly shown using a reliability model like this. The relationship between a structure's components must be discussed when the system reliability of the structure is under consideration.

This study aims to determine a typical TLP's system reliability. As was previously mentioned, a series of reliability considerations can be made for each element of the object platform. As a result, the system reliability of the object platform can be determined using a series reliability method.

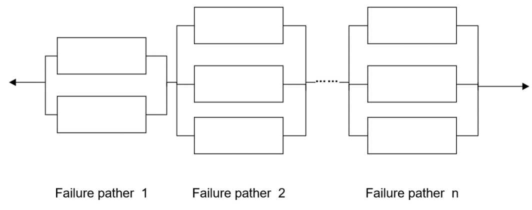

Fig. 6. Failure model of structural system

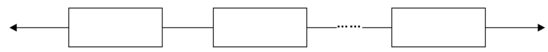

Fig. 7. Failure model at level 1

The failure model at level 1 for a system with a series structure is thought to be accurate and efficient, as shown in Fig. 7. For the majority of structures, the correlation of failure paths is crucial. Each failure path is considered independent if its correlations are in series, as shown by the correlations in the following equation.

Generally speaking, the entire platform can be broken down into various parts. Progressive analysis under the typical hydrodynamic loads revealed that some structural elements failed prior to the total collapse of the structure. An actual case of a structural failure is the collapse of the Alexander L. Kielland platform [19], which was pushed for just 14 minutes before collapsing due to a crack in the main-brace. As a result, the failure of one component directly affects the failure of the entire structure, and variations in component failure could result in various failure modes for the entire structure. The system reliability model for TLP is shown in Fig. 7, which exhibits that the deck, column, pontoon, and two different types of main nodes make up the entire platform.

4.2. Ultimate bearing capacity of TLP

The stress control section of the TLP platform mobilizes its yield strength when the environmental load reaches a threshold value, and the internal force of the section stops increasing as the load does. At this point, the platform is thought to have reached its bearing capacity and some areas have undergone plastic deformation. However, it is believed that material non-linearity is separate from geometrical non-linearity. As a result, the stop of increase in internal force of the control section with increasing external load was taken as the criterion of the limit state in this study when analyzing the ultimate bearing capacity of the platform.

TLP can be in either an operational or survived con-

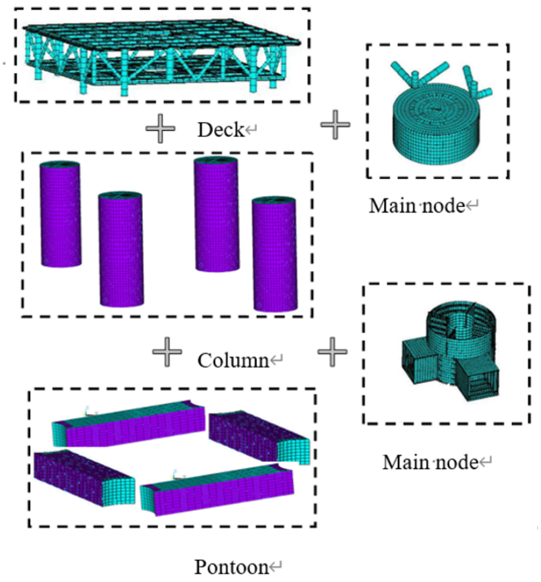

Fig. 8. System reliability model of TLP

dition for the duration of the platform structure's service life. Whereas the latter is more detrimental than the former and ought to be given priority. The South Chinese Sea's wave steepness was used in this study to determine the design wave parameters using the design wave method suggested in DNV and ABS rules. The load cases 14 in Table 2 represent longitudinal extrusion, oblique compression, maximum acceleration, and topside shearing, respectively. The ultimate limit state is also shown in Fig. 4, where Fig. 4(a) illustrates the longitudinal extrusion failure, Fig. 4(b) presents the oblique compression failure, Fig. 4(c) shows the maximum acceleration failure, and Fig. 4(d) exhibts the topside shearing failure. In order to perform a numerical simulation, the wave parameters listed in Table 2 were used. The section load (moment) of the platform was calculated using the post-process tool of ANSYS, and detailed information about these loads (moments) is shown in Tables 3 and 4.

4.3. Statistical properties of random variables

The reliability analysis of the TLP platform contains a lot of unknowns. The limit state equation of the structure can reflect these uncertainties using random variables. The reliability evaluation of the TLP is directly impacted by the probability and statistics of random variables. Therefore, the ultimate load capacity of the platform and the probability and statistical characteristics of the marine environment loads play a significant role in the reliability assessment.

The term FPSOs/FSUsv refers to the probability and statistical properties of additional random variables in the

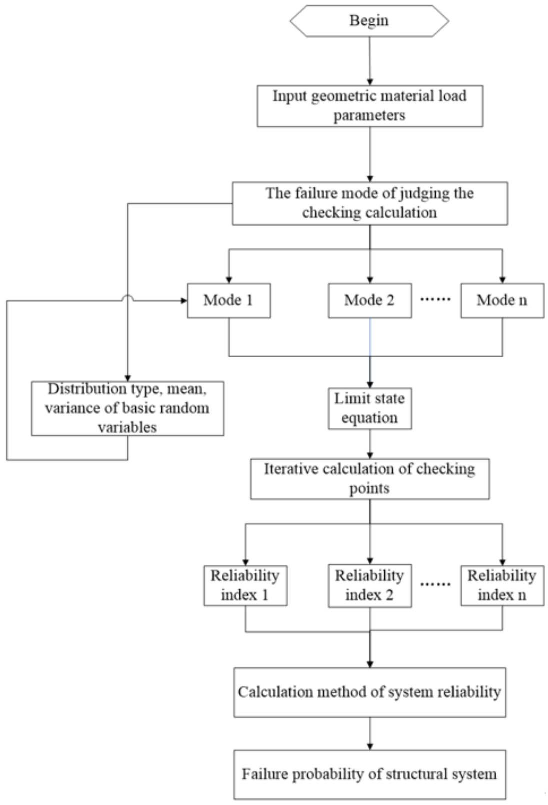

Fig. 9. System reliability analysis procedure of TLP

limit state equation [5]. Table 5 displays the statistics and probability of the random variables.

5. Case study

The reliability computation flowchart used in this study is shown in Fig. 8. Following the establishment of the FEM and the selection of the critical wave loads, the failure mode was ascertained using the FEM, and the limit state function was then derived. As shown in Fig. 7, the parameters of the limit state function were subsequently established in order to compute the probability distribution of each load case for the reliability assessment of various structural components. The reliability assessment of the completed system was then made using the reliability index computed for the system's key components.

Shao Jing-hua et al. [20] proposed method also took the dependability of the effect of main nodes into consideration. The buoy-column junction's horizontal, vertical, and bending moments, as well as the column's shear and bending moments and its maximum shear force in the z-direction, were among the various types of ultimate limit states of local nodes that were taken into account.

The reliability of each component of each subjected load

Table 3. Ultimate cross section internal force

Section load type			
Topsides shearing (kN)	Column bending (kN.m)	Pontoon tension (kN)	Tension leg tension (kN)
6237	0.2502 × 1012	0.7024 × 106	0.1688 × 104

Table 4. Calculation results of load case 1 ∼ 4 under 100 return period

Load Case number	Corresponding load condition	Section Load type (kN or kN.m)	Calculation value
1	Longitudinal extrusion	Topsides shearing	0
		Column bending	0.35575 × 108
		Pontoon tension	0.30100 × 103
		Tension leg tension	0.19240 × 104
2	Oblique compression	Topsides shearing	0
		Column bending	0.12029 × 1012
		Pontoon tension	0.19 × 102
		Tension leg tension	0.25538 × 105
3	Maximum acceleration	Topsides shearing	0
		Column bending	0.21189 × 107
		Pontoon tension	0.1833 × 103
		Tension leg tension	0.38674 × 106
4	Topside shearing	Topsides shearing	2850
		Column bending	0.14028 × 108
		Pontoon tension	0.68096 × 103
		Tension leg tension	0.69438 × 105

Table 5. Failure function stochastic model

Variable	Distribution Type	COV	Mean
R_u	Lognormal	0.08	Calculate
S_w	Gumbel Extreme	0.163	Calculate
γ_u	Normal	0.1	1
γ_w	Normal	0.1	1
γ_m	Normal	0.1	1

case and the system reliability of the TLP were calculated using computer program code based on the first order reliability method (FORM) in accordance with the analysis procedure suggested in this paper as shown in Fig. 8. Table 6 displays the complete results.

The reliability of each load case was roughly equal to that of the dominant failure mode, as shown by the results of Table 6. The two most crucial reliability index values were found to be 2.4 for longitudinal extrusion and maximin acceleration. The other two cases are very similar, with the exception of these two. The system reliability indices demonstrated the method of design wave analysis's logic as well.

6. Conclusion

An effective method for evaluating the system reliability of TLP is presented in this paper. The issue of a TLP under extreme sea states is first taken into consideration. Uncertainty affects the yield stress of the members, which are assumed to fail either in tension or compression, and the entire structure is modeled as a three-dimensional shell model. Environmental loading includes self-weight, buoyancy, current-wave forces, and applied loads, with a generalized extreme value distribution fitting the probability density function of the wave height. After that, a generalized framework for risk assessment is discussed, created, and applied to a typical TLP. According to the proportion method, which is a standard procedure in the structural field, dominant failure modes were identified. As a result, the TLP platform's predominant failure modes can be quickly determined. Finally, a series system model based on the TLP failure mechanism performs the evaluation process while taking into account the statistical dependence between both the components and the failure modes.

References

[1] None, (1983) *"Application of Reliability Methods in Design and Analysis of Offshore Platforms"* **Journal of Structural Engineering *109***(10): 2265–2291. DOI: 10.1061/(ASCE)0733-9445(1983)109:10(2265).

[2] Y. L. Wu and T. Moan, (1991) *"An incremental load formulation for limit states in the reliability analysis of nonlinear systems"* **Structural Safety *10***(4): 307–325. DOI: 10.1007/978-3-642-84753-0_30.

Table 6. System reliability indexes of the target platform

Section load type	Load case 1		2		3		4	
	β	P_f	β	P_f	β	P_f	β	P_f
Platform shearing	7.8	0	7.8	0	7.8	0	3.0	1.4×10^{-4}
Column bending	7.8	0	2.8	1.7×10^{-3}	7.8	0	7.8	0
Pontoon Bending	6.1	0	7.7	0	7.7	0	3.4	2.0×10^{-4}
Tension leg platform	7.8	0	7.5	0	2.4	8.2×10^{-3}	7.0	0
Main nodes	2.4	8.2×10^{-3}	3.7	3.7×10^{-4}	3.9	5×10^{-5}	7.8	7.8
Whole structure	2.4	8.2×10^{-3}	2.8	1.7×10^{-3}	2.4	8.2×10^{-3}	3.0	1.4×10^{-3}

[3] H. H. Sun and Y. Bai, (2003) *"Time-variant reliability assessment of FPSO hull girders"* ***16***(3): 219–253.

[4] C. G. Soares, M. Dogliani, C. Ostergaard, G. Parmentier, and P. T. Pedersen, (1996) *"Reliability based ship structural design"* **Transactions - Society of Naval Architects and Marine Engineers**:

[5] K. Purnendu, B. Das, et al., (2004) *"Structural reliability framework for FPSOs/FSUs [R]"* **Glasgow: Universities of Glasgow and Strathclyde**:

[6] Y. He, L.-K. Xu, Q. Ye, Y.-H. Jiang, and W.-L. Jin. "Reliability-based assessment on stiffened panel of deep-water platform". English. In: **2**. Honolulu, HI, United states, 2009, 621–627.

[7] Y. M. Low, (2009) *"Frequency domain analysis of a tension leg platform with statistical linearization of the tendon restoring forces"* **Marine Structures 22**(3): 480–503.

[8] Young-Joo, Lee, Junho, and Song, (2012) *"Finite-element-based system reliability analysis of fatigue-induced sequential failures"* **Reliability engineering & system safety *108***: 131–141. DOI: 10.1016/j.ress.2012.05.007.

[9] Q. Ye, W.-L. Jin, Y. He, and Y. Bai, (2013) *"System reliability of a semi-submersible drilling rig"* **Ships and Offshore Structures *8***(1): 84–93. DOI: 10.1080/17445302.2011.647806.

[10] L. Hui. *"Tension leg platform hydrodynamic response and global strength research"*. (Master's thesis). Harbin Engineering University, 2012.

[11] Fa-suo, Yan, Da-gang, Zhang, Li-ping, SunYang-shan, and Dai, (2009) *"Stress verification of a TLP under extreme wave environment"* **Journal of Marine Science & Application**: DOI: 10.1007/s11804-009-8105-1.

[12] R. Jin, Y. Jiang, W. Shen, H. Zhang, and B. Geng, (2021) *"Coupled dynamic response of a tension leg platform system under waves and flow at different heading angles: An experimental study"* **Applied Ocean Research *115***(2): 102848. DOI: 10.1016/j.apor.2021.102848.

[13] M. N. Coccon, J. Song, S.-Y. Ok, and U. Galvanetto, (2017) *"A new approach to system reliability analysis of offshore structures using dominant failure modes identified by selective searching technique"* **KSCE Journal of Civil Engineering *21***(6): 2360–2372. DOI: 10.1007/s12205-016-1192-z.

[14] G. U. Jia-Yang, L. Hai-Ning, and J. M. Yang, (2013) *"Studies on coupling dynamic response of TLP in stochastic waves"* **Chuan Bo Li Xue/Journal of Ship Mechanics**: DOI: 10.3969/j.issn.1007-7294.2013.08.007.

[15] J.-y. Gu, J.-m. Yang, and H.-n. Lv, (2012) *"Studies of TLP dynamic response under wind, waves and current"* **China ocean engineering *26***: 363–378. DOI: 10.1007/s13344-012-0028-y.

[16] J.-Y. Gu, H.-N. Lv, and J.-M. Yang, (2012) *"Studies on coupling dynamic response and characteristics of mooring system of TLP in stochastic waves"* **Ocean Engineering(Haiyang Gongcheng) *30***(4): 42–48.

[17] P. Thoft-Christensen and Y. Murotsu, (1989) *"Application of Structural System Reliability Theory"* **Journal of the American Statistical Association *84***(406):

[18] R. E. Melchers and A. Beck. *Structural reliability analysis and prediction*. John wiley & sons, 2018.

[19] A. A. Naess, P. J. Haagensen, B. Lian, T. Moan, and T. Simonsen. "Investigation of the Alexander L. Kielland Failure - Metallurgical and Fracture Analysis". In: *Offshore Technology Conference*. 1982. DOI: 10.1115/1.3231014.

[20] H. D. Shao Jing-hua He Yong, X. Long-kun, and J. Wei-liang, (2012) *"Reliability analysis method for local components of tension leg platform"* **Ocean Engineering *30***(1): 25–32.